Original article

Biomechanical mapping of the female pelvic floor: changes with age, parity and weight

VLADIMIR EGOROV[1], VINCENT LUCENTE[2], HEATHER VAN RAALTE[3], MILES MURPHY[2], SONYA EPHRAIN[2], NINA BHATIA[3], NOUNE SARVAZYAN[1]

[1] *Artann Laboratories, Trenton, United States*
[2] *The Institute for Female Pelvic Medicine & Reconstructive Surgery, Allentown, United States*
[3] *Princeton Urogynecology, Princeton, United States*
Contact email: vegorov@artannlabs.com

Abstract: Quantitative biomechanical characterization of pelvic supportive structures and functions in vivo is thought to provide insight into the pathophysiology of pelvic floor disorders including pelvic organ prolapse (POP). An innovative approach - vaginal tactile imaging - allows biomechanical mapping of the female pelvic floor to quantify tissue elasticity, pelvic support, and pelvic muscle functions. The objective of this study is to explore an extended set of 52 biomechanical parameters to characterize pelvic floor changes with age, parity, and subject weight for normal pelvic floor conditions. 42 subjects with normal pelvic conditions (no POP, no stress urinary incontinence) were included in the data analysis from an observational, case-controlled study. The Vaginal Tactile Imager (VTI) was used with an analytical software package to automatically calculate 52 biomechanical parameters for 8 VTI test procedures (probe insertion, elevation, rotation, Val-salva maneuver, voluntary muscle contractions in 2 planes, relaxation, and reflex contraction). The ranges, mean values, and standard deviations for all 52 VTI parameters were established. 12 VTI parameters were identified as statistically sen-sitive ($p < 0.05$; t-test) to the subject age; 9 parameters were identified as statistically sensitive ($p < 0.05$; t-test) to the sub-ject parity; no sensitivity was found to subject weight. Among the 12 parameters sensitive to women's age, 6 parameters show changes (decrease) in tissue elasticity and 6 parameters show weakness in pelvic muscle functions with age. Among the 9 parameters sensitive to parity, 5 parameters show changes (decrease) in tissue elasticity and 4 parameters show weakness in pelvic muscle functions after giving birth. The biomechanical mapping of the female pelvic floor with the VTI provides a unique set of parameters characterizing pelvic changes with age and parity. These objectively measurable biomechanical transformations of pelvic tissues, support structures, and functions may be used in future research and practical applications.

Keywords: Biomechanical mapping; Female pelvic floor; Aging, Parity, Tactile imaging; Tissue elasticity, Pelvic sup-port, Pelvic function, Elastography,

INTRODUCTION

Many pelvic floor disorders including POP, stress urinary incontinence (SUI), sexual dysfunction, congenital anomalies, and others are clearly manifested in the mechanical properties of pelvic organs [1–4]. Therefore, biomechanical mapping of the response to applied pressure or loads within the pelvic floor opens up new possibilities in biomechanical assessment and monitoring of pelvic floor conditions. The newly developed vaginal tactile imaging technique allows biomechanical mapping of the female pelvic floor including assessment of tissue elasticity, pelvic support, and pelvic muscle functions in high definition [5, 6].

Previously, we reported the intra- and inter-observer reproducibility of vaginal tactile imaging [7] and proposed interpretation of biomechanical mapping of the female pelvic floor [8]. The new mechanistic parameters were introduced for assessment of the vaginal [9] and pelvic floor conditions [10].

The objective of this study is to identify an extended set of Vaginal Tactile Imager (VTI) parameters for biomechanical mapping of the female pelvic floor, to establish parameter ranges, and to explore their sensitivity to age, parity and patient weight for normal pelvic floor conditions.

MATERIALS AND METHODS

Definitions

Tactile Imaging is a medical imaging modality translating the sense of touch into a digital image [9]. The tactile image is a function of $P(x, y, z)$, where P is the pressure on soft tissue surface under applied deformation and x, y and z are the coordinates where P was measured. The tactile image is a pressure map on which the direction of tissue deformation must be specified.

Functional Tactile Imaging translates muscle activity into dynamic pressure pattern $P(x, y, t)$ for an area of interest, where t is time and x and y are coordinates where pressure P was measured. It may include: (a) muscle voluntary contraction, (b) involuntary reflex contraction, (c) involuntary relaxation, and (d) specific maneuvers.

Biomechanical Mapping = Tactile Imaging + Functional Tactile Imaging

A tactile imaging probe has a pressure sensor array mounted on its face that acts similar to human fingers during a clinical examination, deforming the soft tissue and detecting the resulting changes in the pressure pattern on the surface. The sensor head is moved over the surface of the tissue to be studied, and the pressure response is evaluated at multiple locations along the tissue. The results are used to generate 2D/3D images showing pressure distribution over the area of the tissue under study.

Generally, an inverse problem solution for tactile image $P(x, y, z)$ would allow the reconstruction of tissue elasticity distribution (E) as a function of the same coordinates $E(x, y, z)$. Unfortunately, the inverse problem solution is hardly possible for most real objects because it is a non-linear and ill-posed problem. However, the tactile image $P(x, y, z)$ per se reveals tissue or organ anatomy and elasticity distribution because it maintains the stress-strain relationship for deformed tissue [11, 12]. Thus the spatial gradients $\partial P(x, y, z)/\partial x$, $\partial P(x, y, z)/\partial y$, and $\partial P(x, y, z)/\partial z$ can be used in practice for soft tissue elasticity mapping, despite structural and anatomical variations [6].

Vaginal Tactile Imager

The VTI, model 2S (Advanced Tactile Imaging, Inc., NJ), was used in all test procedures. The VTI probe, as shown

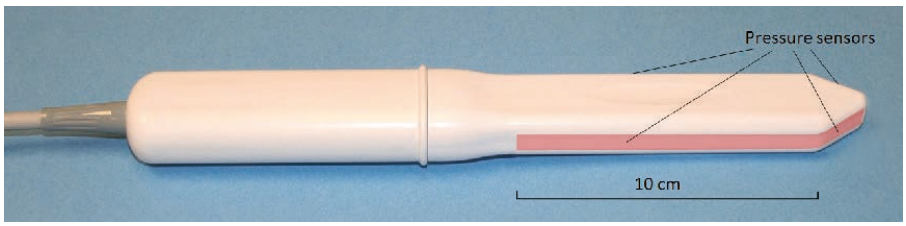

Figure 1. - Vaginal Probe. Pressure sensors are aligned on the outer surfaces of the probe (highlighted in the image).

in Figure 1, is equipped with 96 pressure (tactile) sensors spaced at 2.5 mm consecutively on both sides of the probe, an orientation sensor, and temperature controllers to provide the probe temperature close to a human body before the examination. During the clinical procedure, the probe is used to acquire pressure responses from two opposite vaginal walls along the vagina. The VTI data are sampled from the probe sensors and displayed on the VTI monitor in real time. The resulting pressure maps (tactile images) of the vagina integrate all the acquired pressure and positioning data for each of the pressure sensing elements. Additionally, the VTI records the dynamic contraction for pelvic floor muscles with resolution of 1 mm. A lubricating jelly is used for patient comfort and to provide reproducible boundary/contact conditions with deformed tissues.

This VTI probe allows 3 - 15 mm tissue deformation at the probe insertion (Tests 1), 20 - 45 mm tissue deformation at the probe elevation (Test 2), 5 - 7 mm deformation at the probe rotation (Test 3) and recording of dynamic responses at pelvic muscle contractions (Tests 4 - 8). The probe maneuvers in Tests 1 - 3 allow accumulation of multiple pressure patterns from the tissue surface to compose an integrated tactile image for the investigated area using a proprietary image composition algorithm similar to the imaging of the prostate and breast [11, 12]. The spatial gradients $\partial P\,(x, y) / \partial y$ for anterior and posterior compartments are calculated within the acquired tactile images in Tests 1 and 2; *y*-coordinate is directed orthogonally from the vaginal channel, x-coordinate is located on the vaginal channel. The VTI software includes data analysis tools and reporting functions. It visualizes the anatomy, pressure maps, and calculates (automatically) 52 VTI parameters for eight test procedures. The VTI examination procedure consists of eight tests: 1) probe insertion, 2) elevation, 3) rotation, and 4) Valsalva maneuver, 5) voluntary muscle contraction, 6) voluntary muscle contraction (left *versus* right side), 6) involuntary relaxation, and 8) reflex muscle contraction (cough). Tests 1 - 5 and 7 - 8 provide data for anterior/posterior compartments; test 7 provides data for left/right sides.

The VTI absolute measurement accuracy is as follows: ±0.2 kPa within 10 kPa range, ±0.5 kPa at 25 kPa, ±1.0 kPa at 60 kPa. The VTI relative pressure measurement accuracy lies in the range between ±0.05 kPa to ±0.1 kPa. The VTI pressure measurement resolution is 0.001 kPa. The VTI absolute measurement accuracy for probe orientation is ±0.5 degree and ±0.1°C for measuring the temperature inside the probe on the surface of the pressure sensors. The VTI probe was calibrated immediately before every subject examination; it was cleaned and disinfected between the patients.

Biomechanical Mapping Parameters

Table 1 lists 52 biomechanical parameters being calculated for every participating subject based on VTI data recorded in tests 1 - 8. Anatomical assignment of the targeting/contributing pelvic structures into the specified parameters is based on published data [1, 3, 4, 13-15].

Population Description

42 subjects with normal pelvic conditions (no POP, no SUI) were inlcuded in the data analysis from multi-site ob-

Table 1. VTI Biomechanical Parameters.

No.	VTI Test	Parameters Abbreviation	Units	Parameter Description	Parameter Interpretation	Parameter Class	Targeting/Contributing Pelvic Structures
1	1	Fmax	N	Maximum value of force measured during the VTI probe insertion [9]	Maximum resistance of anterior *vs* posterior widening; tissue elasticity at specified location (capability to resist to applied deformation)	Maximum vaginal tissue elasticity at specified location	Tissues behind the anterior and posterior vaginal walls at 3-15 mm depth
2	1	Work	mJ	Work completed during the probe insertion (Work = Force × Displacement) [9]	Integral resistance of vaginal tissue (anterior and posterior) along the probe insertion	Average vaginal tissue elasticity	Tissues behind the anterior and posterior vaginal walls at 3-15 mm depth
3	1	Gmax_a	kPa/mm	Maximum value of anterior gradient (change of pressure per anterior wall displacement in orthogonal direction to the vaginal channel)	Maximum value of tissue elasticity in anterior compartment behind the vaginal at specified location	Maximum value of anterior tissue elasticity	Tissues/structures in anterior compartment at 10-15 mm depth
4	1	Gmax_p	kPa/mm	Maximum value of posterior gradient (change of pressure per posterior wall displacement in orthogonal direction to the vaginal channel)	Maximum value of tissue elasticity in posterior compartment behind the vaginal at specified location	Maximum value of posterior tissue elasticity	Tissues/structures in anterior compartment at 10-15 mm depth
5	1	Pmax_a	kPa	Maximum value of pressure per anterior wall along the vagina	Maximum resistance of anterior tissue to vaginal wall deformation	Anterior tissue elasticity	Tissues/structures in anterior compartment
6	1	Pmax_p	kPa	Maximum value of pressure per posterior wall along the vagina	Maximum resistance of posterior tissue to vaginal wall deformation	Posterior tissue elasticity	Tissues/structures in posterior compartment
7	2	P1max_a	kPa	Maximum pressure at the area of pubic bone (anterior, A1 in Figure 2)	Proximity of pubic bone to vaginal wall and perineal body strength	Anatomic aspects and tissue elasticity	Tissues between vagina and pubic bone; perineal body
8	2	P2max_a	kPa	Maximum pressure at the area of urethra (anterior, A2 in Figure 2)	Elasticity/mobility of urethra	Anatomic aspects and tissue elasticity	Urethra and surrounding tissues
9	2	P3max_a	kPa	Maximum pressure at the cervix area (anterior, A3 in Figure 2)	Mobility of uterus and conditions of uterosacral and cardinal ligaments	Pelvic floor support	Uterosacral and cardinal ligaments
10	2	P1max_p	kPa	Maximum pressure at the perineal body (posterioir, see P1 in Figure 2)	Pressure feedback of Level III support	Pelvic floor support	Puboperineal, puborectal muscles

11	2	P2max_p	kPa	Maximum pressure at middle third of vagina (posterioir, see P2 in Figure 2)	Pressure feedback of Level II support	Pelvic floor support	Pubovaginal, puboanal muscles
12	2	P3max_p	kPa	Maximum pressure at upper third of vagina (posterioir, see P3 in Figure 2)	Pressure feedback of Level I support	Pelvic floor support	Iliococcygeal muscle, levator plate
13	2	G1max_a	kPa/mm	Maximum gradient at the area of pubic bone (anterior, see A1 in Figure 2)	Vaginal elasticity at pubic bone area	Anterior tissue elasticity	Tissues between vagina and pubic bone; perineal body
14	2	G2max_a	kPa/mm	Maximum gradient at the area of urethra (anterior, see A2 in Figure 2)	Mobility and elasticity of urethra	Urethral tissue elasticity	Urethra and surrounding tissues
15	2	G3max_a	kPa/mm	Maximum gradient at the cervix area (anterior, see A3 in Figure 2)	Conditions of uterosacral and cardinal ligaments	Pelvic floor support	Uterosacral and cardinal ligaments
16	2	G1max_p	kPa/mm	Maximum gradient at the perineal body (posterioir, see P1 in Figure 2)	Strength of Level III support (tissue deformation up to 25 mm)	Pelvic floor support	Puboperineal, puborectal muscles
17	2	G2max_p	kPa/mm	Maximum gradient at middle third of vagina (posterioir, see P2 in Figure 2)	Strength of Level II support (tissue deformation up to 35 mm)	Pelvic floor support	Pubovaginal, puboanal muscles
18	2	G3max_p	kPa/mm	Maximum gradient at upper third of vagina (posterioir, see P3 in Figure 2)	Strength of Level I support (tissue deformation up to 45 mm)	Pelvic floor support	Iliococcygeal muscle, levator plate
19	3	Pmax	kPa	Maximum pressure at vaginal walls deformation by 7 mm [9]	Hard tissue or tight vagina	Vaginal tissue elasticity	Tissues behind the vaginal walls at 5-7 mm depth
20	3	Fap	N	Force applied by anterior and posterior compartments to the probe [9].	Integral strength of anterior and posterior compartments	Vaginal tightening	Tissues behind anterior/ posterior vaginal walls.
21	3	Fs	N	Force applied by entire left and right sides of vagina to the probe [9].	Integral strength of left and right sides of vagina	Vaginal tightening	Vaginal right/left walls and tissues behind them.
22	3	P1_l	kPa	Pressure response from a selected location (irregularity 1) at left side (see S1 in Figure 2)	Hard tissue on left vaginal wall	Irregularity on vaginal wall	Tissue/muscle behind the vaginal walls on left side.
23	3	P2_l	kPa	Pressure response from a selected location (irregularity 2) at left side (see S2 in Figure 2)	Hard tissue on left vaginal wall	Irregularity on vaginal wall	Tissue/muscle behind the vaginal walls on left side.
24	3	P3_r	kPa	Pressure response from a selected location (irregularity 3) at right side (see S1 in Figure 2)	Hard tissue on right vaginal wall	Irregularity on vaginal wall	Tissue/muscle behind the vaginal walls on right side.
25	4	dF_a	N	Integral force change in anterior compartment at Valsalva maneuver	Pelvic function* at Valsalva maneuver	Pelvic function	Multiple pelvic muscle*
26	4	dPmax_a	kPa	Maximum pressure change in anterior compartment at Valsalva maneuver.	Pelvic function* at Valsalva maneuver	Pelvic function	Multiple pelvic muscle*
27	4	dL_a	mm	Displacement of the maximum pressure peak in anterior compartment	Mobility of anterior structures* Valsalva maneuver	Pelvic function	Urethra, pubovaginal muscle; ligaments*
28	4	dF_p	N	Integral force change in posterior compartment at Valsalva maneuver	Pelvic function* at Valsalva maneuver	Pelvic function	Multiple pelvic muscle*
29	4	dPmax_p	kPa	Maximum pressure change in posterior compartment at Valsalva maneuver.	Pelvic function* at Valsalva maneuver	Pelvic function	Multiple pelvic muscle*
30	4	dL_p	mm	Displacement of the maximum pressure peak in posterior compartment	Mobility of posterioir structures* Valsalva maneuver	Pelvic function	Anorectal, puborectal, pubovaginal muscles; ligaments*
31	5	dF_a	N	Integral force change in anterior compartment at voluntary muscle contraction	Integral contraction strength of pelvic muscles along the vagina	Pelvic function	Puboperineal, puborectal, pubovaginal and ilicoccygeal muscles; uretra
32	5	dPmax_a	kPa	Maximum pressure change in anterior compartment at voluntary muscle contraction	Contraction strength of specified pelvic muscles	Pelvic function	Puboperineal, puborectal and pubovaginal muscles
33	5	Pmax_a	kPa	Maximum pressure value in anterior compartment at voluntary muscle contraction.	Static and dynamic peak support of the pelvic floor	Pelvic function	Puboperineal and puborectal muscles*
34	5	dF_p	N	Integral force change in posterior compartment at voluntary muscle contraction	Integral contraction strength of pelvic muscles along the vagina	Pelvic function	Puboperineal, puborectal, pubovaginal and ilicoccygeal muscles
35	5	dPmax_p	kPa	Maximum pressure change in posterior compartment at voluntary muscle contraction	Contraction strength of pelvic muscles at specified location	Pelvic function	Puboperineal, puborectal and pubovaginal muscles
36	5	Pmax_p	kPa	Maximum pressure value in posterior compartment at voluntary muscle contraction.	Static and dynamic peak support of the pelvic floor	Pelvic function	Puboperineal and puborectal muscles*
37	6	dF_r	N	Integral force change in right side at voluntary muscle contraction	Integral contraction strength of pelvic muscles along the vagina	Pelvic function	Puboperineal, puborectal, and pubovaginal muscles
38	6	dPmax_r	kPa	Maximum pressure change in right side at voluntary muscle contraction	Contraction strength of specific pelvic muscle	Pelvic function	Puboperineal or puborectal or pubovaginal muscles
39	6	Pmaxa_r	kPa	Maximum pressure value in right side at voluntary muscle contraction	Specified pelvic muscle contractive capability and integrity	Pelvic function	Puboperineal or puborectal muscles
40	6	dF_l	N	Integral force change in left side at voluntary muscle contraction	Integral contraction strength of pelvic muscles along the vagina	Pelvic function	Puboperineal, puborectal, and pubovaginal muscles
41	6	dPmax_l	kPa	Maximum pressure change in left side at voluntary muscle contraction	Contraction strength of specific pelvic muscle	Pelvic function	Puboperineal or puborectal or pubovaginal muscles
42	6	Pmaxa_l	kPa	Maximum pressure value in left side at voluntary muscle contraction	Specified pelvic muscle contractive capability and integrity	Pelvic function	Puboperineal or puborectal muscles
43	7	dPdt_a	kPa/s	Anterior absolute pressure change per second for maximum pressure at involuntary relaxation	Innervation status of specified pelvic muscles	Innervations status	Levator ani muscles
44	7	dpcdt_a	%/s	Anterior relative pressure change per second for maximum pressure at involuntary relaxation	Innervation status of specified pelvic muscles	Innervations status	Levator ani muscles
45	7	dPdt_p	kPa/s	Posterior absolute pressure change per second for maximum pressure at involuntary relaxation	Innervation status of specified pelvic muscles	Innervations status	Levator ani muscles
46	7	dpcdt_p	%/s	Posterior relative pressure change per second for maximum pressure at involuntary relaxation	Innervation status of specified pelvic muscles	Innervations status	Levator ani muscles

47	8	dF_a	N	Integral force change in anterior compartment at reflex pelvic muscle contraction (cough)	Integral pelvic function* at reflex muscle contraction	Pelvic function	Multiple pelvic muscle*
48	8	dPmax_a	kPa	Maximum pressure change in anterior compartment at reflex pelvic muscle contraction (cough).	Contraction strength of specified pelvic muscles	Pelvic function	Multiple pelvic muscle*
49	8	dL_a	mm	Displacement of the maximum pressure peak in anterior compartment	Mobility of anterior structures* at reflex muscle contraction	Pelvic function	Urethra, pubovaginal muscle; ligaments*
50	8	dF_p	N	Integral force change in posterior compartment at reflex pelvic muscle contraction (cough)	Integral pelvic function* at reflex muscle contraction	Pelvic function	Multiple pelvic muscle*
51	8	dPmax_p	kPa	Maximum pressure change in posterior compartment at reflex pelvic muscle contraction (cough).	Contraction strength of specified pelvic muscles	Pelvic function	Multiple pelvic muscle*
52	8	dL_p	mm	Displacement of the maximum pressure peak in posterior compartment	Mobility of anterior structures* at reflex muscle contraction	Pelvic function	Anorectal, puborectal and pubovaginal muscles; ligaments*

** requires further interpretation*

servational, case-controlled study (clinical trial identifier NCT02294383). The subject age, height, weight, and parity distribution data are present in Table 2. Prior to the VTI examination, a standard physical examination was performed, including a bimanual pelvic examination and Pelvic Organ Prolapse Quantification (POP-Q) [16]. None of the analyzed subjects had a prior history of pelvic floor surgery. The clinical protocol was approved by the Institutional Review Board and all women provided written informed consent to be enrolled into the study. This clinical research was done in compliance with the Health Insurance Portability and Accountability Act. The VTI examination data for eight Tests were obtained and recorded at the time of the scheduled routine urogynecologic visits.

Total study workflow comprised of the following steps: (1) Recruiting women who routinely undergo vaginal examination as a part of their diagnostic treatment of concerned areas; (2) Acquisition of clinical diagnostic information related to the studied cases by standard clinical means; (3) Performing a VTI examination in lithotomic position; (4) Analyzing VTI data and assessment of the VTI parameters for pelvic floor characterization.

Statistical Analysis

52 biomechanical parameters were calculated automatically per each of the 42 analyzed VTI examinations or cases (one VTI examination per each subjects). In some rare cases the parameter calculation required a manual correction of the anatomical location where the parameters must be calculated. Unpaired *t*-tests between two subject groups with thresholds by age, parity or subject weight were completed per parameter to determine whether the parameter showed dependence on the age, parity or subject weight. For visual evaluation of the analyzed clinical data distributions we used notched boxplots [17] showing a confidence interval for the median value (central horizontal line), 25% and 75% quartiles. The spacing between the different parts of the box helps to compare variance. The boxplot also determines skewness (asymmetry) and outlier (cross). The intersection or divergence of confidence intervals for two patient samples is a visual analog of the *t*-test. The MATLAB (MathWorks, MA) statistical functions were used for the data analysis. The MATLAB (MathWorks, MA) statistical functions were used for the data analysis.

Figure 2 shows the locations of the measured VTI parameters for test 2 and 3 in mid-sagittal plane of the female pelvic floor.

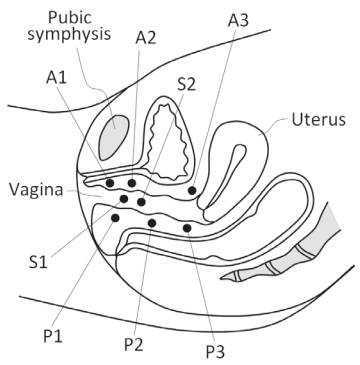

Figure 2. - Locations of the VTI parameters within the pelvic floor. A1-A3 are in anterior compartment (Test 2), P1-P3 in posterior compartment (Test 2), and S1, S2 are in lateral compartments (left and right sides, Test 3).

RESULTS

To illustrate the approach and location used in calculating the biomechanical parameters, the VTI examination data for all eight tests, as they observed by an operator in real time, are displayed in Figures 4 - 11 (see Supplementary material). Table 2 displays the calculated statistics (hypothesis testing outcome *H*- and *p*-value) for two age groups with threshold of 52 y.o. Average values for 52 biomechanical parameters and standard deviations (SD) for both groups are presented. Table 4 presents the calculated statistics (hypothesis testing outcome *H*- and *p*-value) for nulliparous *versus* parous (Parity > 0) woment, two parity groups average values and standard deviations for 52 biomechanical parameters.

Calculated statistics (hypothesis testing outcome *H*- and *p*-value) for two weight groups with threshold of 69 kg demonstrated no sensitivity to women weight; $H = 0$ and $p > 0.316$ for all 52 biomechanical parameters.

The *t*-tests for the age groups demonstrate that 12 out of 52 parameters have statistically significant differences between the groups and that these parameters have the potential to be used for identification of age-related changes in the female pelvic floor (see Table 2). The analysed groups, statistically, have the same subject height, weight, and parity distributions ($H = 0$, $p>0.05$). The *t*-tests for the parity groups demonstrate that 9 out of 52 parameters have statistically significant differences between the groups and that these parameters have the potential to be used for the identification of parity changes in the female pelvic floor (see Table 3). The analysed groups also statistically have the same subject height, weight and age distributions ($H = 0$, $p>0.05$). The *t*-tests for the weight groups demonstrate that o out of 52 parameters have statistically significant differences between the groups; nothing changes with women's weight (see Table 3). The analysed groups thus statistically have the same subject height, age and parity distributions ($H = 0$, $p>0.05$).

Figure 3 displays the boxplots for select parameters for the age groups presented in Table 2 (panels A - D) and for parity groups presented in Table 3 (panels E - H).

Table 2. Biomechanical Parameters for two age groups: Group 1 of 26 subjects ≤52 y.o., Group 2 of 16 subjects >52 y.o.

		H	*p*	Units	Average Group 1	Average Group 2	SD Group 1	SD Group 2
	Height →	0	0.315	cm	163.1	159.3	10.1	14.3
	Weight →	0	0.177	kg	60.4	80.8	6.8	6.1
	Age →	1	**1×10^{-12}**	**y.o**	**40.7**	**68.3**	8.3	9.0
	Parity (P) →	0	0.117	-	1.23	1.75	0.99	1.06
Parameters number ↓	**Test ↓**							
1	1	1	0.016	N	1.46	0.90	0.80	0.48
2	1	1	0.009	mJ	49.23	31.14	23.41	15.79
3	1	0	0.103	kPa/mm	2.82	1.67	2.65	0.84
4	1	0	0.196	kPa/mm	1.74	1.29	1.21	0.78
5	1	0	0.263	kPa	43.10	33.48	29.90	20.24
6	1	1	0.047	kPa	26.07	17.07	16.27	8.15
7	2	0	0.490	kPa	26.96	30.33	14.04	17.02
8	2	0	0.534	kPa	12.44	10.89	8.21	6.98
9	2	0	0.648	kPa	8.96	7.78	6.70	10.03
10	2	0	0.077	kPa	15.86	10.45	11.19	5.14
11	2	0	0.914	kPa	9.45	9.68	7.23	5.03
12	2	0	0.198	kPa	8.14	4.99	9.22	3.24
13	2	0	0.488	kPa/mm	1.74	2.12	1.74	1.54
14	2	0	0.794	kPa/mm	0.76	0.83	0.76	0.99
15	2	0	0.610	kPa/mm	0.62	0.51	0.58	0.81
16	2	0	0.057	kPa/mm	0.93	0.39	1.06	0.40
17	2	0	0.763	kPa/mm	0.40	0.43	0.29	0.32
18	2	0	0.107	kPa/mm	0.56	0.25	0.74	0.18
19	3	0	0.562	kPa	33.27	30.37	15.42	15.99
20	3	0	0.120	N	4.40	3.45	2.14	1.34
21	3	0	0.073	N	1.37	0.90	0.90	0.60
22	3	1	0.003	kPa	11.43	5.60	7.10	2.02
23	3	1	0.012	kPa	5.87	3.42	3.52	1.55
24	3	1	0.001	kPa	12.29	5.91	6.93	2.48
25	4	0	0.128	N	1.44	1.02	0.94	0.53
26	4	0	0.717	kPa	11.28	9.90	12.38	9.07
27	4	0	0.558	mm	2.31	1.28	4.68	5.47
28	4	0	0.094	N	1.46	0.94	1.06	0.56
29	4	0	0.350	kPa	7.73	5.76	7.02	4.78
30	4	0	0.299	mm	1.44	3.44	4.46	6.49
31	5	0	0.248	N	1.71	1.35	1.09	0.79
32	5	0	0.124	kPa	25.15	17.58	16.43	12.79
33	5	0	0.259	kPa	43.52	36.54	20.97	15.76
34	5	0	0.070	N	2.11	1.39	1.36	0.96
35	5	1	0.024	kPa	16.45	9.66	10.58	5.98
36	5	1	0.009	kPa	26.06	17.39	11.59	6.51
37	6	0	0.056	N	1.03	0.63	0.62	0.59
38	6	1	0.019	kPa	9.70	5.04	6.33	4.80
39	6	1	0.004	kPa	16.62	8.99	8.41	6.16
40	6	0	0.110	N	1.01	0.64	0.70	0.67
41	6	1	0.031	kPa	8.61	4.71	5.57	4.80
42	6	1	0.002	kPa	15.81	7.86	8.48	5.51
43	7	0	0.501	kPa/s	-1.45	-1.08	1.82	1.37
44	7	0	0.618	%/s	-3.36	-2.76	3.79	3.31
45	7	0	0.195	kPa/s	-1.27	-0.68	1.60	0.87
46	7	0	0.785	%/s	-4.26	-3.91	4.24	3.37
47	8	0	0.138	N	2.59	1.83	1.44	1.33
48	8	0	0.990	kPa	13.91	13.97	14.27	16.30
49	8	0	0.530	mm	6.99	5.91	3.91	5.66
50	8	0	0.062	N	2.68	1.69	1.42	1.46
51	8	0	0.096	kPa	13.55	8.66	7.94	8.01
52	8	0	0.723	mm	4.01	3.19	6.03	6.90

Table 3. Biomechanical Parameters for two groups: Group 1 of 11 nulliparous subjects, Group 2 of 31 subjects with parity ≥1.

		H	*p*	Units	Aver Group 1	Aver Group 2	SD Group 1	SD Group 2
Height →		0	0.843	cm	161.1	161.9	13.8	11.3
Weight →		0	0.587	kg	147.5	152.6	25.1	27.2
Age →		0	0.185	y.o	45.6	53.1	15.2	16.1
Parity (P) →		1	**1×10^{-11}**	-	**0.0**	**1.9**	0.0	0.7
Parameters number ↓	**Test ↓**							
1	1	1	0.034	N	1.65	1.10	1.08	0.53
2	1	0	0.141	mJ	50.95	39.29	29.43	19.08
3	1	0	0.072	kPa/mm	3.41	2.01	3.18	1.66
4	1	0	0.651	kPa/mm	1.69	1.52	0.61	1.21
5	1	0	0.347	kPa	46.04	37.09	36.63	22.61
6	1	0	0.291	kPa	26.61	21.24	11.45	15.14
7	2	0	0.497	kPa	25.54	29.20	5.00	17.35
8	2	0	0.427	kPa	10.24	12.42	6.22	8.20
9	2	0	0.511	kPa	7.12	9.00	4.79	8.92
10	2	0	0.321	kPa	16.31	12.91	9.10	9.82
11	2	0	0.826	kPa	9.16	9.67	6.88	6.35
12	2	0	0.397	kPa	8.64	6.34	12.46	5.11
13	2	1	0.020	kPa/mm	0.90	2.23	0.44	1.79
14	2	0	0.100	kPa/mm	0.43	0.92	0.44	0.92
15	2	0	0.343	kPa/mm	0.41	0.63	0.28	0.76
16	2	0	0.579	kPa/mm	0.86	0.68	0.73	0.96
17	2	0	0.221	kPa/mm	0.51	0.38	0.38	0.26
18	2	0	0.197	kPa/mm	0.64	0.37	1.03	0.36
19	3	0	0.464	kPa	35.15	31.10	15.42	15.65
20	3	0	0.332	N	4.52	3.86	2.00	1.89
21	3	0	0.061	N	1.59	1.05	0.81	0.80
22	3	0	0.144	kPa	11.63	8.35	5.98	6.36
23	3	1	0.006	kPa	7.09	4.17	4.16	2.32
24	3	1	0.042	kPa	13.22	8.67	6.16	6.19
25	4	0	0.218	N	1.55	1.14	1.14	0.66
26	4	0	0.891	kPa	11.10	10.48	13.25	10.25
27	4	0	0.284	mm	3.51	1.31	5.04	4.99
28	4	0	0.505	N	1.40	1.16	1.23	0.78
29	4	0	0.960	kPa	6.90	6.77	7.11	5.86
30	4	0	0.541	mm	3.45	2.06	4.69	5.79
31	5	0	0.216	N	1.89	1.46	1.51	0.73
32	5	1	0.047	kPa	30.17	19.46	21.62	11.79
33	5	0	0.064	kPa	50.08	37.58	22.65	17.14
34	5	0	0.313	N	2.17	1.72	1.74	1.06
35	5	0	0.360	kPa	16.17	13.04	12.72	8.36
36	5	0	0.322	kPa	25.55	21.76	12.30	10.18
37	6	1	0.034	N	1.27	0.74	0.87	0.51
38	6	0	0.096	kPa	10.88	6.80	7.34	5.55
39	6	0	0.093	kPa	17.71	12.11	7.65	8.25
40	6	1	0.008	N	1.42	0.69	1.13	0.45
41	6	1	0.044	kPa	10.39	5.97	7.05	4.76
42	6	0	0.072	kPa	17.03	11.09	8.73	7.82
43	7	0	0.975	kPa/s	-1.31	-1.29	1.55	1.68
44	7	0	0.993	%/s	-3.11	-3.10	3.22	3.70
45	7	0	0.868	kPa/s	-0.94	-1.03	0.80	1.47
46	7	0	0.666	%/s	-4.64	-3.96	3.65	3.94
47	8	0	0.406	N	2.63	2.13	1.15	1.51
48	8	0	0.153	kPa	20.51	11.74	8.12	16.14
49	8	0	0.796	mm	6.90	6.39	3.20	5.16
50	8	0	0.437	N	2.61	2.12	1.31	1.56
51	8	0	0.404	kPa	13.55	10.70	6.20	8.78
52	8	1	0.049	mm	7.44	2.39	9.71	4.32

DISCUSSION

The results of this research agree with previously reported data [4-10]; however, the current analysis includes the biggest VTI parameter set ever considered. 12 of 52 biomechanical parameters are identified as having statistically significant sensitivity to the women's age (see Tables 2). Their average changes are from 49.9% to 107.8% (78.2% in average). 9 of 52 biomechanical parameters are identified as having statistically significant sensitivity to women's parity (see Tables 3). Their average changes are from 49.6% to 211% (83.2% in average). These changes with age and parity clearly outperform possible deviations related to VTI intra- and inter-operator variability which were found on an average of ±15.1% (intra-observer error) and ±18.4 (inter-observer error) [7]. These reproducibility errors have value and sign intrinsically by a chance, but we have identified statistically systematic parameter changes by age and parity. No parameter changes were found with the women weight.

Let's consider the age changes. Test 1 provides three identified age-sensitive parameters (1, 2, 6) related to tissue elasticity; their average values is changed by 52.8% - 67.18% (see panels A – C in Figure 3). No changes in pelvic support, which could be detected by Test 2 parameters were found. Test 3 provides three identified parameters (22, 23, 24) related to the tissue elasticity of side vaginal walls and beyond 3-7 mm (small irregularities); their average values change from 71.6% to 108%. Pelvic muscle contraction Tests 5 and 6 provide six identified parameters (35, 36, 38, 39, 41, 42) related to pelvic function; their average values are changed by 49.9% - 101.2% (see panel D in Figure 3). All these 6 parameters demonstrate a decrease in muscle contractive capabilities in Level I (levator plate muscle) and Level II support (pubovaginal and ilicoccygeal muscles). Valsalva maneuver (Test 4), involuntary muscle relaxation (Test 7), and reflex muscle contraction at cough (Test 8) demonstrated no changes in parameters with age. In total, among the 12 age parameters, 6 parameters are related to decrease in vaginal tissue elasticity and 6 parameters are related to pelvic function – the weakened muscle contractive strength with age.

Let's consider the parity changes. Test 1 provides one parity-sensitive parameter (1) related to tissue elasticity; its average value changes by 49.6% (see panel E in Figure 3). This parameter is the maximum resistance force the VTI probe insertion. This maximum resistance comes from the perineal body which deteriorates after giving birth. No changes in pelvic support (Test 2) were found except for parameter 13, which increased with the parity (see panel F in Figure 3). This, at first sight, is an unexpected result and might be easily explained by significant softening of tissues between the vaginal wall and the pubic bone. As a result, these soft tissues demonstrate an increased pressure gradient to the bone due to their low resistance to displacement *versus* that of the bone. It means that parameter 13 changes with parity and relates to the tissue elasticity change rather than to pelvic support. Test 3 provides two identified parameters (23, 24) related to tissue elasticity at the side of vaginal walls and beyond 3-7 mm (small irregularities); their average values change by 70.1% and 52.5%. With regards to pelvic muscle contraction, Tests 5 and 6 provides four identified parameters (32, 37, 40, 41) related to pelvic function; their average values are changed by 55.0% - 105.5% (see parameter 37 change in Figure 3, panel G). These changes in pelvic muscle contractive strength must be related to avulsed puborectalis [15]. Valsalva maneuver (Test 4), involuntary muscle relaxation (Test 7), and the reflex muscle contraction at cough (Test 8) demonstrated no changes with the parity. In total, among the 9 age parameters, 5 parameters are related to a decrease in vaginal tissue elasticity and 4 parameters are related to pelvic function – the weakened muscle contractive strength (avulsion) with the parity.

It is important to note that the subject sample analysed in this study with normal pelvic conditions (no POP, no SUI) was composed of the visitors of urogynecological site; these patients may have had some pelvic floor conditions that were not identified in this study. Possibly, the patients from the normal group had pre-prolapse conditions which hadn't yet transformed into anatomically visible POP. This study reasonably proposes that if more subjects with no history of consulting urogynecological clinics would be added to this sample, more significant differences in the VTI parameters with regards to age and parity may be observed.

The next step (which falls beyond the purview of this article) with these biomechanical parameters may include (a) an insight into POP *versus* normal pelvic conditions, (b) an insight into POP classes (anterior *versus* posterior *versus* uterine), (c) analysis for continence *versus* incontinence conditions, (d) analysis of urogynecological surgical outcomes as a whole as well as per specific surgical procedure, (e) a combination of VTI data with urodynamics, ultrasound, and MRI data, (f) the usage of the VTI and other clinically related data for predicative modelling of outcomes for conservative and surgical procedures (personalized predictive treatment), and (g) maintenance of the objective history of biomechanical transformation of the patient pelvic floor.

One of the strengths of this study is that the current VTI offers an opportunity to assess tissue elasticity, pelvic support structures, and pelvic function (muscle and ligaments) in high definition along the entire length of the anterior, posterior, and lateral walls at rest with applied deflection pressures and pelvic muscle contractions. All 52 parameters are calculated automatically in real-time. This allows a large body of measurements to evaluate individual variations in support defects as well as identify specific problematic structures. In addition, the technology provides the opportunity to measure pelvic floor muscle strength at specific locations along the vaginal wall and helps correlate its relative contributions to measured tissue properties. These measurements may provide insight into the functional contribution or relationship between support ligaments and the underlying muscle support. Because VTI testing is relatively easy and inexpensive to obtain, post-treatment follow-up is available to evaluate the surgical impact on functional tissue properties and pelvic floor muscles. This may provide valuable outcome measurements for evaluating current and future treatments.

One of the shortcomings of this study is its relatively small sample size. Further studies with larger patient populations, investigating varieties of other pelvic floor conditions and their use in the evaluation of interventions including physical therapy, conservative management options, and surgical correction are needed to further explore the diagnostic values of biomechanical mapping of the female pelvic floor.

CONCLUSIONS

The biomechanical mapping of the female pelvic floor with the VTI provides a unique set of parameters characterizing pelvic changes with age and parity. These objectively measurable biomechanical transformations of pelvic tissues, support structures and functions may be used in future research and practical applications.

ACKNOWLEDGEMENTS

Research reported in this publication was supported by the National Institute On Aging of the National Institutes of Health under Awards Number R44AG034714 and SB1AG034714. The content is solely the responsibility of

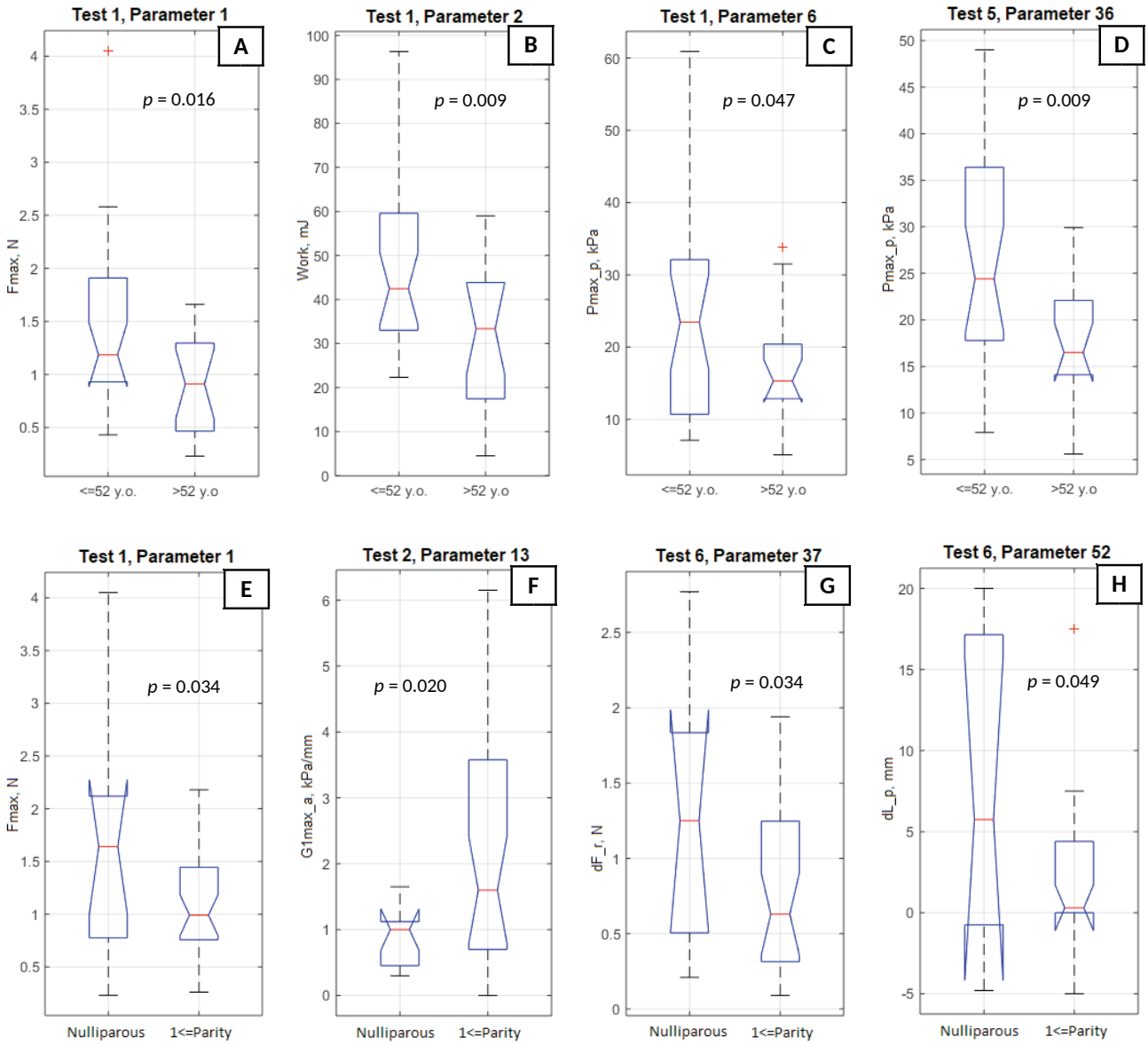

Figure 3. - Boxplots A - D for selected biomechanical parameters for the age groups and boxplots E – H for selected biomechanical parameters for the parity groups.

the authors and does not necessarily represent the official views of the National Institutes of Health.

DISCLOSURE

V. Egorov: CEO and shareholder of Advanced Tactile Imaging, Inc.
H. van Raalte: shareholder of Advanced Tactile Imaging, Inc.

REFERENCES

1. Petros P. The Female Pelvic Floor: Function, Dysfunction and Management According to the Integral Theory. 3rd ed. Berlin, Germany: Springer; 2010: 1–330.
2. Siddiqui NY, Gregory WT, Handa VL, DeLancey JOL, Richter HE, Moalli P, Barber MD, Pulliam S, Visco AG, Alperin M, Medina C, Fraser MO, Bradley CS. American Urogynecologic Society Prolapse Consensus Conference Summary Report. Female Pelvic Med Reconstr Surg. 2018 Jan 5. PMID: 29309287 [Epub ahead of print]
3. DeLancey JO. Pelvic floor anatomy and pathology. In: Hoyte L, Damaser MS, editors. Biomechanics of the Female Pelvic Floor. 1st ed. London, UK: Elsevier; 2016: 13–51.
4. Egorov V, van Raalte H, Lucente V. Quantifying vaginal tissue elasticity under normal and prolapse conditions by tactile imaging. International Urogynecology Journal 2012; 23(4): 459-466.
5. Egorov V, van Raalte H, Sarvazyan A. Vaginal Tactile Imaging. IEEE Transactions on Biomedical Engineering 2010; 57(7): 1736-1744.
6. Egorov V, van Raalte H, Lucente V, Sarvazyan A. Biomechanical characterization of the pelvic floor using tactile imaging. In: Biomechanics of the Female Pelvic Floor, Eds. Hoyte L, Damaser MS, 1st Edition, Elsevier, 2016: 317-348.
7. van Raalte H, Lucente V, Ephrain S, Murphy M, Bhatia N, Sarvazyan N, Egorov V. Intra- and inter-observer reproducibility of vaginal tactile imaging. Female Pelvic Medicine & Reconstructive Surgery 2016; 22(5S): S130-131.
8. Lucente V, van Raalte H, Murphy M, Egorov V. Biomechanical paradigm and interpretation of female pelvic floor conditions before a treatment. International Journal of Women's Health 2017; 9: 521-550.
9. van Raalte H. Egorov V. Tactile imaging markers to characterize female pelvic floor conditions. Open Journal of Obstetrics and Gynecology 2015; 5: 505-515.
10. Egorov V, Murphy M, Lucente V, van Raalte H, Ephrain S, Bhatia N, Sarvazyan N. Quantitative Assessment and Interpretation of Vaginal Conditions. Sexual Medicine 2018; 6(1): 39-48.
11. Egorov V, Ayrapetyan S, Sarvazyan AP. Prostate Mechanical

Imaging: 3-D Image Composition and Feature Calculations. IEEE Transactions on Medical Imaging 2006; 25(10): 1329-40.
12. Egorov V, Sarvazyan AP. Mechanical imaging of the breast. IEEE Trans Med Imaging 2008; 27(9): 1275-87.
13. Shobeiri SA. Practical Pelvic Floor Ultrasonography. A Multicompartmental Approach to 2D/3D/4D Ultrasonography of the Pelvic Floor, 2nd Edition, Springer International Publishing AG, 2017: 1-368.
14. Dietz HP. Pelvic Floor Ultrasound. Atlas and Text Book. Creative Commons Attribution License. Springwood, Australia; 2016: 1–127.
15. Hoyte L, Ye W, Brubaker L, Fielding JR, Lockhart ME, Heilbrun ME, Brown MB, Warfield SK. Segmentations of MRI images of the female pelvic floor: a study of inter- and intra-reader reliability. J Magn Reson Imaging 2011; 33(3): 684-91.
16. Bump R.C., Mattiasson A., Bo K. et al. (1996) The standardization of terminology of female pelvic organ prolapse and pelvic floor dysfunction. American Journal of Obstetrics and Gynecology, 175, 10-17.
17. McGill R., Tukey J.W., Larsen W.A. (1978) Variations of Box Plots. American Statistician 32:12–16.

SUPPLEMENTANTARY MATERIAL (ON-LINE)

Figure 4. - A tactile image acquired during the VTI probe insertion (Test 1) with anatomical landmarks and maximum pressure graphs (green lines, kPa) along anterior and posterior compartments.

Figure 5. - A tactile image acquired during the VTI probe elevation (Test 2) with anatomical landmarks and pressure values at specified locations (see A1-A3 and P1-P3 in Figure 2) along anterior and posterior compartments. The VTI software automatically identified all these 6 locations and shows the pressure values and gradient values (nor shown) for these locations.

Figure 6. - A tactile image acquired during the VTI probe rotation (Test 3) with pressure values at specified locations (see S1 and S2 in Figure 2). The VTI software automatically identified all these 3 locations and shows the pressure values (local maximums) for these locations.

Figure 7. - A dynamic pressure patterns acquired during the Valsalva maneuver for anterior and posterior compartments (Test 4).

Figure 8. - A dynamic pressure patterns acquired during the voluntary muscle contraction for anterior and posterior compartments (Test 5).

Figure 9. - A dynamic pressure patterns acquired during the voluntary muscle contraction for left and right vaginal compartments (Test 6).

Figure 10. - A dynamic pressure patterns acquired during the involuntary muscle relaxation for interior and posterior compartments (Test 7).

Figure 11. - A dynamic pressure patterns acquired during the reflex contraction (cough) for anterior and posterior compartments (Test 8).